4 Holocene morphodynamics in the Ugii Nuur basin, Mongolia – insights from a sediment profile and 1D electrical resistivity tomography

Schwanghart, W., Schütt, B. (2008). *Zeitschrift für Geomorphologie*, 52, Suppl. 2, 35-55.

Summary

Sediment profile analysis and electrical resistivity tomography were applied in the Ugii Nuur basin, central Mongolia, in order to gain insight into the sedimentary architecture of valley fillings. It is shown that important constituents in the near surface ground are aeolian fines. Coarse grainsizes were predominantly deposited during the Late Pleistocene and the beginning of the Holocene indicating local dune activity and arid conditions. Since the Early to Mid Holocene a larger proportion of silt suggests an increase in mineral dust deposition. In combination with soil formation this points at dust trapping by a denser vegetation cover that reflects more humid conditions in the Ugii Nuur basin. Yet, 1D electrical resistivity tomography (VES) shows that Holocene deposits represent only a minor part of the thick valley fillings. Hence, it is assumed that there main extent has been established during the Pleistocene.

Zusammenfassung

Im Rahmen einer Studie zur Klima- und Landschaftsgeschichte im Ugii Nuur Einzugsgebiet (zentrale Mongolei) wurde ein Sedimentprofil anhand geochemischer und mineralogischer Verfahren analysiert und geoelektrische Methoden angewendet, um einen Einblick in den Aufbau von Talfüllungen zu bekommen. Es wird gezeigt, dass der oberflächennahe Untergrund durch äolische Ablagerungen dominiert wird. Gröbere Kornfraktionen wurden vorwiegend während des Späten Pleistozäns und dem Beginn des Holozäns abgelagert und

weisen auf lokale Dünenaktivität und aride Bedingungen hin. Deposition von Schluff seit dem Frühen bis Mittleren Holozän lassen auf einen Anstieg in der Deposition mineralischen Staubs schließen. In Kombination mit Bodenbildung weist dies auf eine dichtere Vegetationsdecke hin, die als Staubfänger agiert und feuchtere Bedingungen widerspiegelt. Messungen mit ein-dimensionaler elektrischer Widerstandstomographie (VES) zeigen, dass die Holozänen Ablagerungen nur einen geringen Teil der Talfüllungen einnehmen. Darum wird vermutet, dass die Bildung der mächtigen Talfüllungen vorwiegend während des Pleistozäns stattfand.

Keywords

aeolian deposits, hill wash deposits, calcrete, soil sediments

4.1 Introduction

The Ugii Nuur basin is an ideal location to study Holocene landscape development and climate evolution in the highly continental area of the steppe region of Mongolia. Distinct features of this area are thick layers of debris accumulated and reworked by periglacial, aeolian, fluvial or hill wash processes. The vastness of these debris covers can be especially recognized from air photographs where their extent leaves a mark of a landscape drowning in its own sediments.

The processes generating these debris covers and the temporal placement of their genesis are poorly understood. In this study we investigated the sedimentary architecture of valley fillings by 1D vertical electrical soundings (VES) and a profile description in order to understand the depositional processes and environments in the Ugii Nuur basin. Electrical resistivity tomography is a valuable tool in geomorphological surveys as it provides insight into the structure of the near surface ground (Dahlin, 2001; Kneisel, 2003; Löwner *et al.*, 2005). Most prominently it has been applied in permafrost research – a discipline where electrical soundings benefit from the strong contrast in electrical conductivity between ground ice and overlying debris (Hauck and Vonder Mühll, 2003; Kneisel, 2004, 2005; Krautblatter and Hauck, 2007). Other fields of application are predominantly geoarcheological investigations where buried remnants of walls could be detected in several

meters depths (Piro *et al.*, 2000; Aspinall and Gaffney, 2001). Our investigation aims at the application of this geophysical tool to quantify thickness of valley fillings. The overall goal of the presented work is to contribute to the understanding of the Holocene climate and landscape evolution of todays steppe region of Mongolia.

4.2 State of the Art

The origin of the vast debris cover accumulations has been previously explained by several authors for different areas (Berkey and Morris, 1927; Richter *et al.*, 1963; Haase, 1983; Walther and Naumann, 1997; Grunert *et al.*, 2000; Lehmkuhl and Haselein, 2000; Jadambaa *et al.*, 2003). Grunert *et al.* (2000) and Lehmkuhl and Haselein (2000) describe the thick deposits of unconsolidated debris and fluvial pebble in the Uvs Nuur basin as interfingering alluvial fans and fanglomerates, and indicate them as pediments (*bajadas*). They assume that their formation predominantly occurred during the cold periods of the Pleistocene. Owen *et al.* (1997) and Owen *et al.* (1998) investigated vast alluvial fans prograding from the mountain ranges in the Gobi desert in southern Mongolia. They affiliate their predominant formation to hill wash and fluvial processes during the period from 23 to 9 ky BP, when the climate was more arid, flash flooding dominated and ephemeral streams deposited coarse fanglomerates.

According to Lehmkuhl and Lang (2001) enhanced moisture supply and subsequent denser vegetation cover led to a general reduction in sediment yield during the Early Holocene. Increased moisture availability is recorded in various archives like lake sediments by a rapid increase in lake levels (Walther *et al.*, 2003), which is likely linked to the abrupt monsoon intensification at $\sim$ 11.5 ky BP (Sirocko *et al.*, 1993; Wang *et al.*, 1999; Herzschuh, 2006). Rising lake levels, however, may partly be explained by increased melt water supply from glaciated areas due to increased summer insolation (Walther, 1999; Walther *et al.*, 2003). According to Gunin *et al.* (1999) steppe vegetation dominated at most sites in Mongolia and deserts occupied large depressions in western Mongolia from 11.5 to 8.9 ky BP. Partly, this aridisation resulted in a decrease in lake levels (Walther *et al.*, 2003) and reactivation of dune fields (Grunert *et al.*, 2000).

Mid Holocene ($8.9 - 4.5$ ky BP) records provide an ambivalent picture of Mongolia's

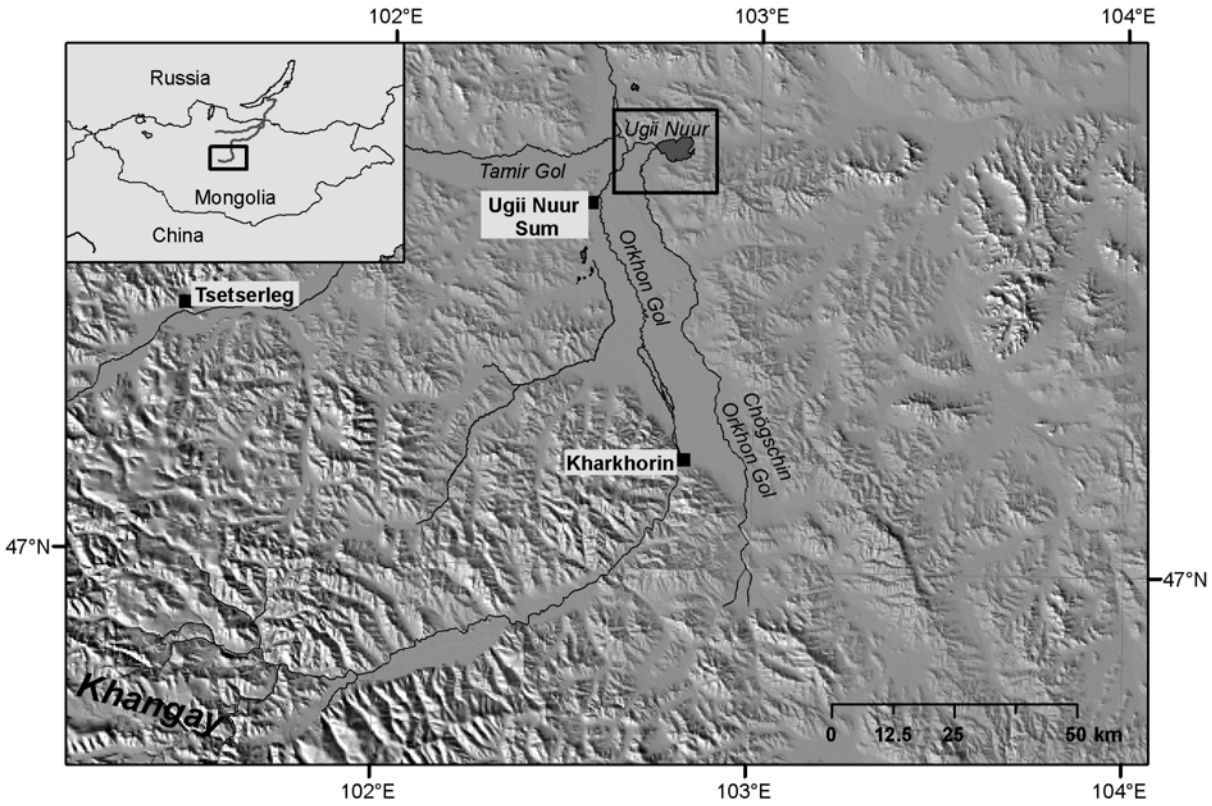

Figure 4.1: Location of the study area. Hillshading is based on SRTM-3 data.

climate during this time. While many areas experienced better moisture conditions (Gunin *et al.*, 1999; Tarasov *et al.*, 2000; Grunert and Dasch, 2004; Yang *et al.*, 2004) with minor fluctuations (Walther *et al.*, 2003), significant aforestation cannot be recognized in most pollen profiles (Gunin *et al.*, 1999; Rösch *et al.*, 2005). Moreover, records of Lake Hovsgol and Baikal (Prokopenko *et al.*, 2007), Lake Telmen (Peck *et al.*, 2002; Fowell *et al.*, 2003) and GCM simulations (Bush, 2005) suggest a trend towards dryer conditions during the Mid Holocene. A prevalence of moisture conditions similar to present since $\sim$ 4 ky BP (Gunin *et al.*, 1999; Prokopenko *et al.*, 2007) is locally interrupted by short dryer and wetter periods (Peck *et al.*, 2002; Fowell *et al.*, 2003; Walther *et al.*, 2003).

At present, ephemeral streams trench the extended debris covers and deposit much smaller fans than those deposited during Pleistocene glacial periods due to a reduction in sediment supply and increased vegetation cover (Lehmkuhl and Haselein, 2000; Lehmkuhl and Lang, 2001). An important constituent in the debris covers is a high content of silt and

fine sands whose origin, on the one hand, is regarded as product of intensified weathering during the glacial stages. On the other hand it has been shown that a horizontal cycle of mobilization of silts and sands deposited in ancient river courses and lake systems, short to long range transport and consecutive deposition by the wind led to a redistribution of these fines during the interstadials (Grunert *et al.*, 2000; Grunert and Lehmkuhl, 2004). Yet, the importance of aeolian processes in the generation of loess like deposits and dune fields is high as investigations on current wind blown dust suggest (Natsagdorj *et al.*, 2003; Dulam, 2005).

4.3 Study site

Ugii Nuur is a quasi-endorheic lake located at 47°44'N and 102°46'E at an elevation of 1328 m (EGM96) (Fig. 4.1, 4.2). The lake is situated at the eastern flank of the Middle Orkhon Valley, which runs in northward direction and is formed by the Orkhon Gol (Orkhon River) in the west and Chögschin Orkhon Gol (Old Orkhon River) in the east. At present, the lake is fed by the Old Orkhon River and episodically drains into the Orkhon River during high lake levels.

The climate of the area is extremely continental and can be described as BSk-climate following the classification concept of KÖPPEN (Kottek *et al.*, 2006). Mean annual air temperature is around 0°C and annual precipitation sums up to 250 mm. A strong seasonality marked by an extremely high annual temperature amplitude and a pronounced contrast between winter and summer precipitation amounts reflect the varying influence of air masses and insolation. While snow depths of 10 cm are hardly exceeded during the winter months, precipitation during July amounts up to 180 mm and often constitutes in strong rainfall events (Barthel, 1983).

Lake Ugii Nuur is located along a graben structure. Tertiary volcanism east of the Ugii Nuur basin points to increased Cenozoic tectonic activity (Walther and Gegeensuvd, 2005). The bedrock mainly consists of Carboniferous, highly fissile mudstones that dip almost perpendicular (Traynor and Sladen, 1995; Sladen and Traynor, 2000; Jadambaa *et al.*, 2003). Cliff lines along Ugii Nuur's southern shoreline expose reddish late Cretacious and Tertiary conglomerates that provide evidence for fluvial dynamics with high bedload

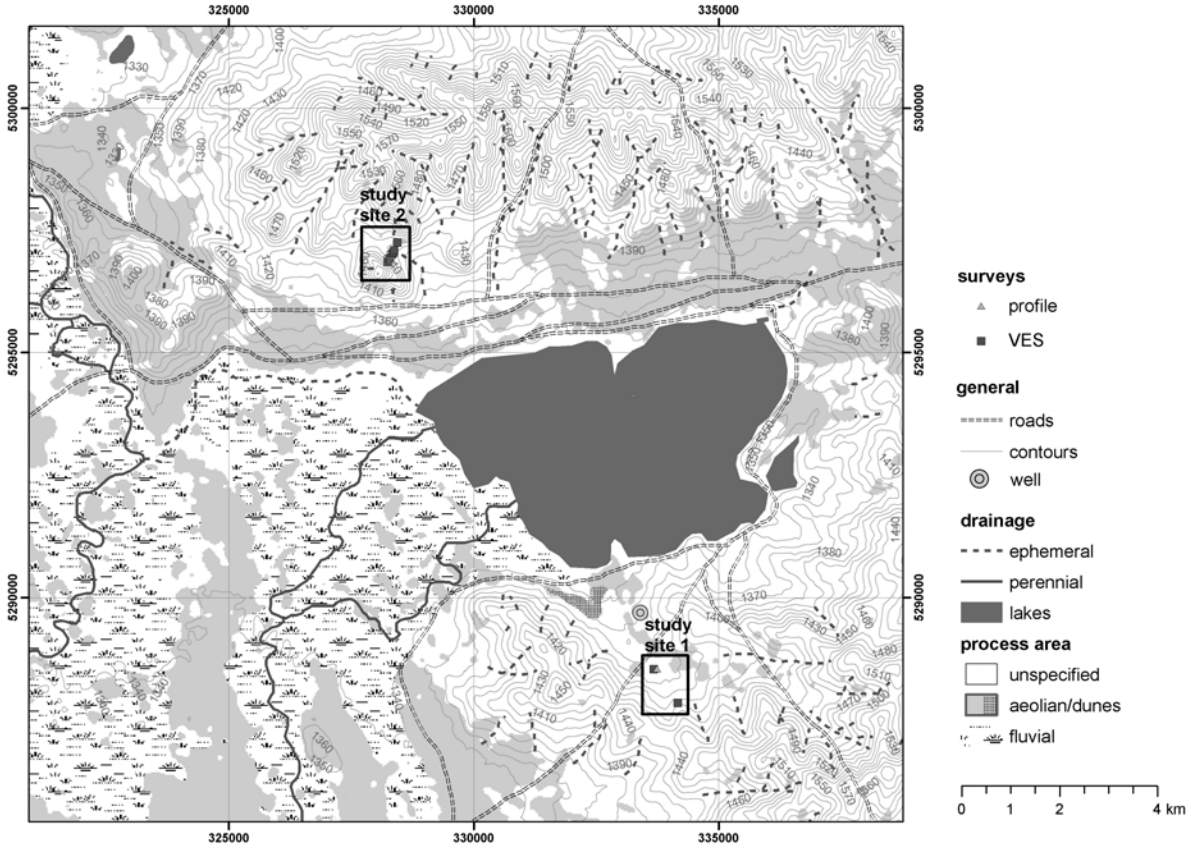

Figure 4.2: Map of the Ugii Nuur basin with locations of the study sites.

transport as documented by pebble beds and channel bar sandstones (Traynor and Sladen, 1995).

Relief differs between the northern and southern part of the basin (Fig. 4.2). The north is characterized by hilly to mountainous terrain with elevations up to 1600 m while the south has a gentle undulating relief with broad saucer-shaped valleys. Both in the northern and southern part of the basin, valleys are filled with thick debris covers reflecting the interfingering influence of slope processes as frost weathering and cryoturbation, solifluction and accumulation of material displaced by hill wash, fluvial accumulation along the channels and wind-driven deposition of a loess-like sediment coverage.

The Ugii Nuur basin is located within the zone of highly continental steppe soil formation (Opp and Hilbig, 2003). Soils found in the Ugii Nuur basin predominantly consist of

Kastanozems (Haase, 1983) while Regosols and Leptosols dominate on steep slopes and ridges. Soils are loamy to sandy riddled with a considerable amount of debris and pebbles that are often layered and adjusted. The study site is situated within the area of dry, gras steppes (Hilbig, 1995; Opp and Hilbig, 2003) and is dominated by grasses (*Cleistogenes*, *Stipa*), forbs (*Allium*), and shrubs (*Artemisia*, *Caragana*) while trees lack throughout the study site.

4.4 Methods

Vertical electrical soundings (VES) were performed using an Oyo McOhm Model 2115A Mark-2. The Schlummberger array geometry with a four electrode configuration was chosen as it is less affected by lateral variations in layer thickness and resistivity (Kneisel, 2003). Current (C) electrode spacings s [m] were increased exponentially by $s(i)/2 = 10i/8\,\mathrm{m}$ with $i = 1, 2, \ldots$ as index of electrode placing. The distance a of the potential (P) electrodes was set to $a/2 = 0.5\,\mathrm{m}$ with $s/2 < 17\,\mathrm{m}$. At larger C electrode spacings the P electrode spacing was increased to $a/2 = 1.5\,\mathrm{m}$. The apparent resistivity φ_a [Ωm] is the product of the measured resistivity R [Ω] and the geometry factor K (Mussett and Khan, 2000). K was calculated by

$$K = \frac{\pi}{a}\left(\left(\frac{s}{2}\right)^2 - \left(\frac{a}{2}\right)^2\right) \tag{4.1}$$

Modeling of vertical apparent resistivity profiles and of inverted layer models (Dahlin, 2001) was performed using the interpretation software ResixIp (Interpex LTD).

A Differential Global Positioning System (DGPS) performing code correction was used to survey landforms. The DGPS was a combination of two Ashtech Mobilemapper Pro™ as rovers and an Ashtech Promark™ as reference station. The software Mobilemapper Office™ was applied to postprocess the data. The DGPS enables the kinematic recording of point, line and area features with submeter accuracy.

Soil profile descriptions were implemented according to the guidelines of AG Bodenkunde (2005), yet, when referring to soil type we refer to the World Reference Base (WRB) system. Samples were taken in 10 cm intervals and age control was gained by three ^{14}C datings conjointly on humins and humic acids by the Poznan Radiocarbon Laboratory. Calibration of radiocarbon dates was accomplished with CalPal, a software for calibration and

visualization developed and distributed by the Prehistory Institute at University Cologne. As calibration curve CalPal2004-SFCP was used.

Sample preparation included drying at 50°C in a drying cabinet and subsequent homogenisation in an agate swing-sledge mill. Prior to chemical analysis sample material was screened and components larger 2 mm were rejected. Total organic carbon (TOC) and inorganic carbon (TIC) content were measured with a carmhograph (Wösthoff) (detection limit = 0.02 weight-% C), organic carbon content was calculated as the difference of both values. Element analysis was performed by inductively coupled plasma atomic emission spectroscopy (ICP-AES, Optima 3000, Perkin Elmer) of the Aqua Regina extracted samples. Loss of ignition was determined at 550°C for the air dried, not homogenized sample.

The mineralogical composition was specified by X-ray powder diffraction analyses using a copper kα-tube from $2 - 52$ °2θ with steps of 0.01 °2θ and each step measured for one minute. Contents of mineral components were recorded semi-quantitativly by the diffraction-intensity at the mineral's major diffraction peak (cps) relatively to the intensity of quartz at its major diffraction peak (d101) from counts per second (cps) whereas 50 cps refers to spurs, $50 - 200$ cps to low, $200 - 500$ cps to low-medium, $500 - 1000$ to medium, $1000 - 2500$ cps to high and > 2500 cps to very high content.

4.5 Results

4.5.1 Study site 1

The first site investigated is located in the southern part of the Ugii Nuur basin in a ca. 3 km broad, saucer-shaped valley running in northwest direction (Fig. 4.2). The relief is gently undulating to almost flat with an absence of forms indicating concentrated surface run-off.

Information on the character of valley infills were derived from an outcrop of 250 cm depth (Fig. 4.3) dug on the south exposed slope in ca. 100 m distance from the depth contour of the valley. The profile's lithology can be subdivided into several distinct layers that have a very high fraction of fine sands in common as indicated by the dominance of quartz and feldspars by XRD (table 4.1). Mica and amphiboles constitute only minor

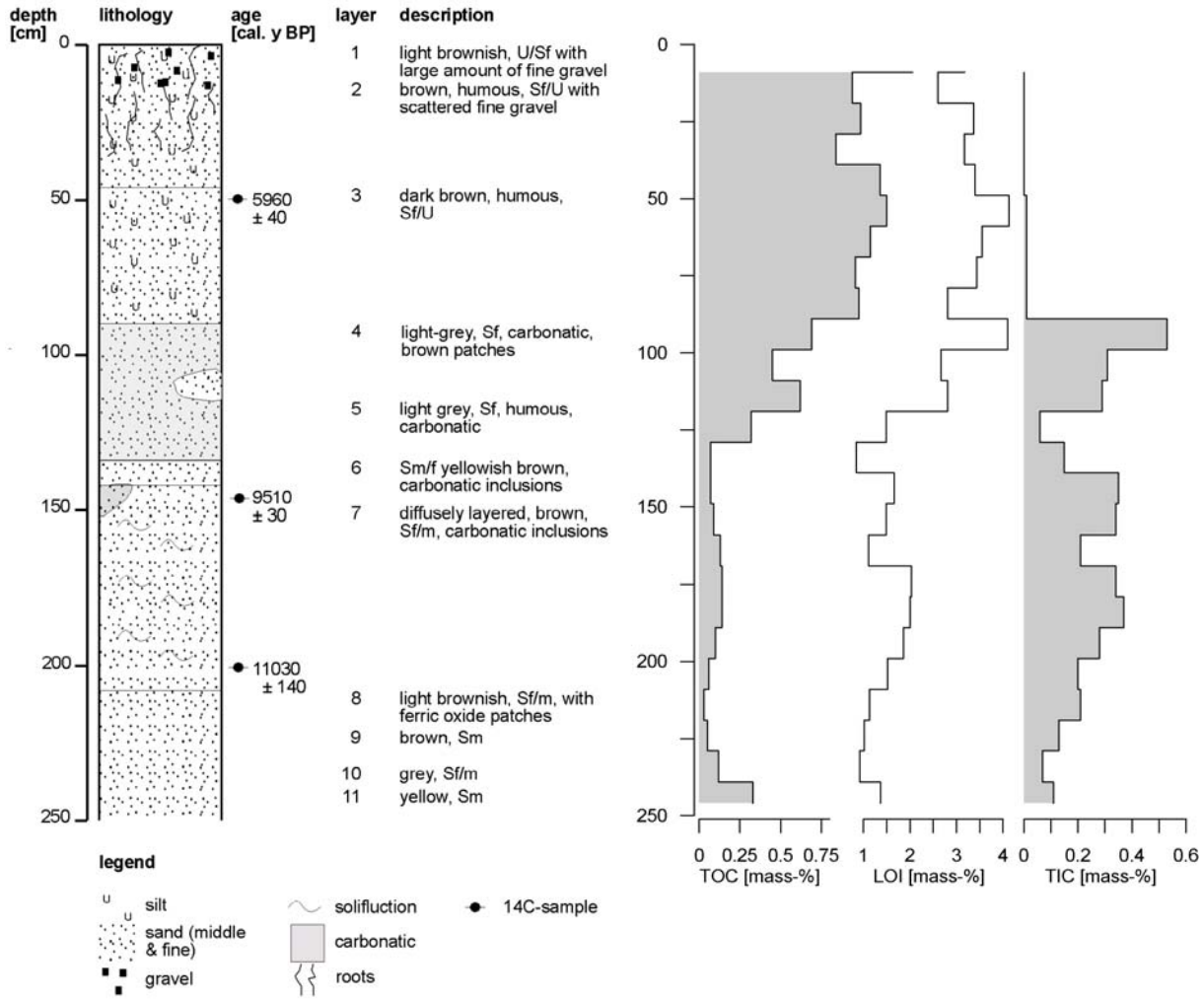

Figure 4.3: Profile description in study site 1 and total inorganic carbon (TIC), total organic carbon (TOC) and loss of ignition (LOI) (see location of the profile in Fig. 4.2).

components of the mineral arrangement in the profile (table 4.1). Soil is classified as Kastanozem with a litter cover of 40–50% and strong rooting to a depth of ca. 45 cm. Root-remnants are partially found down to a depths of 90 cm. The grain size composition in the upper 45 cm of the outcrop can be characterized by the scattered occurrence of fine gravel in a silty to sandy matrix (layers 1, 0–12 cm depth, and 2, 12–45 cm; Fig. 4.3).

Beneath 45 cm sediments change in color from light brown (layer 2, 12–45 cm) to brown (layer 3, 45–90 cm) and to light grey (layer 4, 90–115 cm). Grainsize composition changes from fine sand and silt in layers 3 to fine sands in layer 4 and shows a slight trend with depth toward fine and middle sand. Next to this, layer 3 is characterized by increased TOC

Table 4.1: Loss of ignition (LOI), carbonate content and mineral composition of samples taken in the sediment profile in study site 1.

			minerals[2]				
depth cm	LOI [%]	carbonate content[1] [%]	quartz	feldspars	amphibole	mica	calcite
9	3.18	0	+++++	+++	(+)	(+)	(+)
19	2.60	0	+++++	+++	(+)	(+)	(+)
29	3.37	0	++++	+++	(+)	(+)	(+)
39	3.17	0	++++(+)	+++	(+)	(+)	(+)
49	3.40	0	++++(+)	+++	(+)	(+)	(+)
59	4.13	0.08	++++(+)	+++	(+)	(+)	(+)
69	3.55	0.08	++++	+++	(+)	(+)	(+)
79	3.44	0.08	++++	+++	(+)	(+)	(+)
89	2.81	0.08	++++	+++	(+)	(+)	(+)
99	4.10	4.41	++++	+++	(+)	(+)	+
109	2.67	2.58	++++	++++	(+)	(+)	+
119	2.81	2.42	++++	+++	(+)	+	+
129	1.49	0.5	+++++	+++	(+)	(+)	(+)
139	0.85	1.25	+++++	+++	(+)	(+)	(+)
149	1.66	2.92	+++++	+++	(+)	(+)	(+)
159	1.49	2.83	+++++	+++	(+)	(+)	(+)
169	1.11	1.75	+++++	+++	(+)	(+)	(+)
179	2.03	2.83	+++++	+++(+)	(+)	(+)	(+)
189	2.00	3.08	++++(+)	+++(+)	(+)	(+)	+
199	1.86	2.33	++++(+)	++++	(+)	(+)	(+)
209	1.52	1.67	+++++	+++(+)	+	(+)	(+)
219	1.13	1.75	+++++	+++(+)	(+)	(+)	(+)
229	1.02	1.08	+++++	+++(+)	(+)	(+)	(+)
239	0.92	0.58	+++++	++++	(+)	(+)	+
246	1.37	0.92	+++++	++++	(+)	(+)	+

[1] carbonate content (mass-%) = 8.33 x TIC (mass-%)

[2] estimation of quantity

(+)	traces	+++	medium
+	low	++++	high
++	low-medium	+++++	very high

content that rapidly decreases in layer 4. The transition from layer 3 to 4 is very sharp. From 90-135 cm highly compacted, fine sands prevail, cemented by carbonate (layer 4 and 5) as indicated by reaction when treated with hydrochloric acid. Below layer 5 (115–135 cm), a diffuse transition into a less compacted, 10 cm thick, yellowish brown layer of carbonate free fine sands (layer 6, 135–145 cm) occurs. Beneath, a strangled layer, weakly humous and with carbonatic inclusions shows a brownish color (layer 7, 145–208 cm). This layer is underlain by light brownish fine sand with singular ferric oxide patches in the upper part (layer 8, 208-223 cm, and 9, 223–235 cm). Beneath 235 cm depth sediments are composed of pure fine to middle sand and exhibit a grayish color in layer 10 (235–240 cm) descending into a yellowish color in layer 11 in beneath a depth of 240 cm.

TIC contents along the whole profile are altogether low. Only in layers 4 and 5 TIC peaks at 0.4–0.55 mass-%. Carbonate contents in these layers are calculated to range between 2.4–4.4 mass-% and prevail as calcium carbonate (calcite) as indicated by XRD (table 4.1). While carbonates occur as unlaminated and cemented in layers 4 and 5, they prevail as sparsely scattered concretions in the layers beneath. The chemograph of calcium concentrations shows a similar pattern as the TIC curve throughout the profile.

TOC decreases from top to bottom. At the top TOC totals 1.6 mass-% and decreases in layer 2 to 0.8 mass-%. In layer 3 TOC concentrations show a slight increase to 1.2 mass-%, while in layer 4 TIC concentrations decline again with short term variations. In layer 5 TOC contents increase again and amount 0.5 mass-%. Except for a minor increase at the profile bottom, TOC ranges around 0.1 mass-% below layer 5. A Pearson correlation coefficient of 0.88 indicates a very good correlation of TOC and LOI.

The element composition varies along the profile (Fig. 4.4). Ca and S feature peaks are associated with the aforementioned carbonatic layers 4 and 5. Metals, heavy metals and PO_4 show higher values in the upper part of the core before they tend to decline downward from the uppermost 20 cm. Their concentrations and TOC concentrations are positively correlated (e.g. $r_{TOC,Fe}$, $\alpha < 0.01$, $n = 21$).

A chronological framework of the profile was established by dating three samples in 50, 148 and 198 cm depth (Fig. 4.3). ^{14}C ages constitute 4010 ± 30, 8500 ± 50 and 9670 ± 50 uncal. years, respectively. Calibration against independent estimates of calendar ages

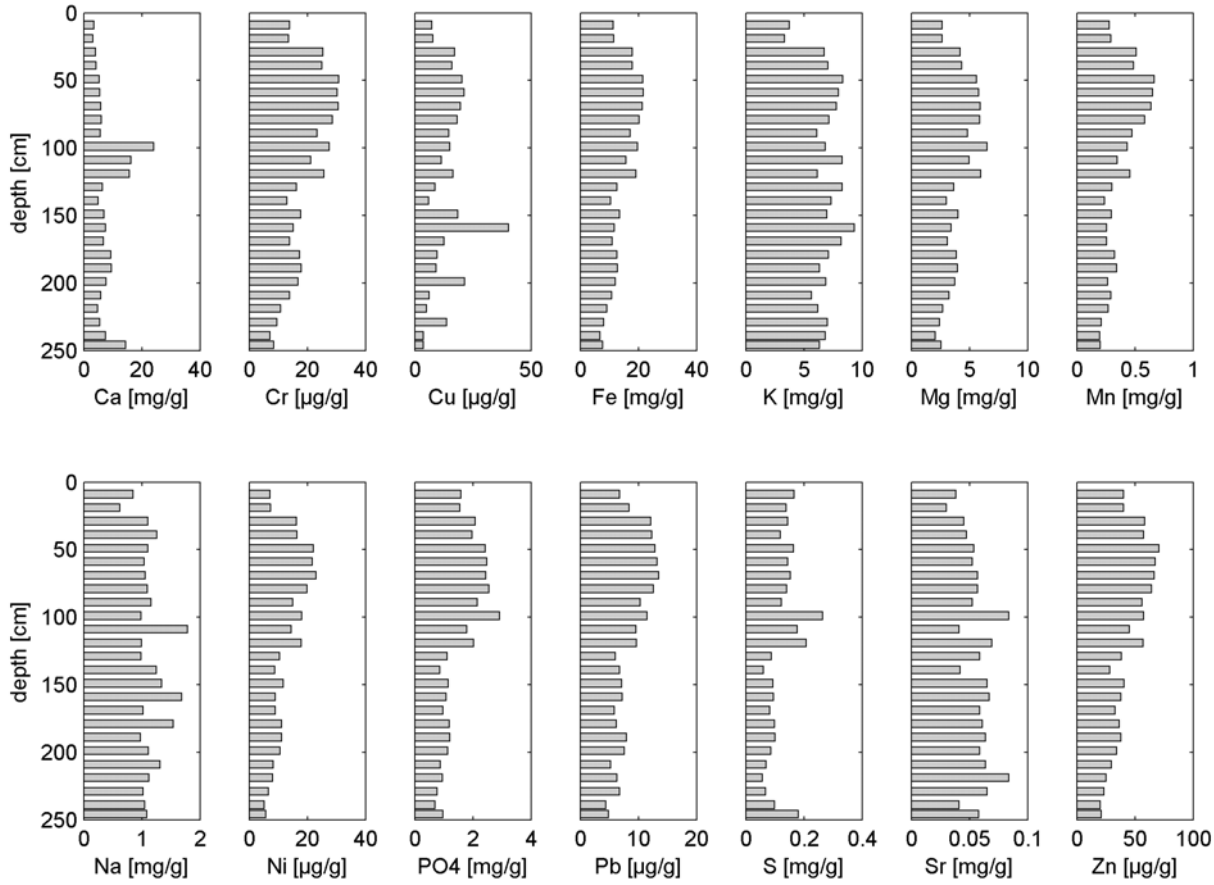

Figure 4.4: Element composition of samples taken in study site 1.

yields 5960 ± 40, 9510 ± 30 and 11030 ± 140 cal. years BP.

Two VES were conducted in the vicinity of the outcrop (Fig. 4.2). VES #1A is located 10 m to the west of the outcrop and, thus, is assumed to reflect the outcrop structure. A four layer model was fit with an error of 2.753 and shows changes in resistivity in 1.5 and 2.3 m, from where a low-impedance layer with a apparent resistivity of 22 Ωm until a depth of 53 m is recognized (Fig. 4.5, #1A). VES #1B is located on a slope adjacent to the outcrop and reflects a shallow weathered layer. Generally higher resistivities are found throughout the profile and with a distinct increase at a depth of 10–11 m below surface (Fig. 4.5, #1B).

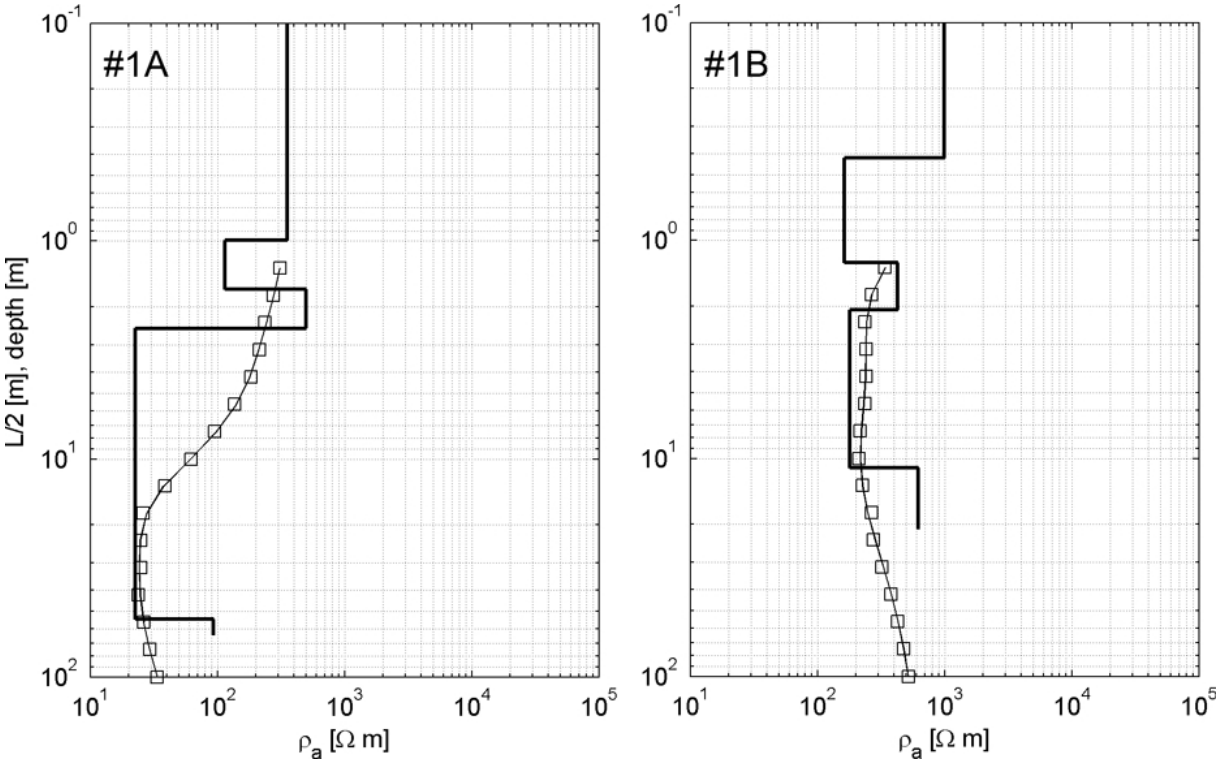

Figure 4.5: One-dimensional electrical resistivity sounding profiles in study site 1.

4.5.2 Study site 2

Study site 2 is located in a valley tributary to a major Ugii Nuur inflow in the northern part of the basin (Fig. 4.2). The cross valley profile runs south-north and depicts a slightly inclined 1100 m wide saucer-shaped valley (Fig. 4.7). While the north-facing concave slope of the cross profile is characterized by a downslope constant rate of inclination change, the south exposed slope features several knickpoints between rather straight slope sections. Although not well resolved by the DGPS measurements, the valley bottom exhibits a small V-shaped drainageway of approximately 3 m width and 1 m depth.

The substrata of the northward exposed slope transforms from schistous bedrock partially covered by blocky debris in a silty to sandy matrix at the hilltop to silty sand with sparse occurrence of boulders and gravel at the valley bottom. The south facing slope experiences a more distinct change in substrata from the valley bottom to the top. Alluvial cones of coarse gravel located at the hillslope base are attached to straight slope sections of exposed bedrock partly covered by boulders and debris. The slope is intermit-

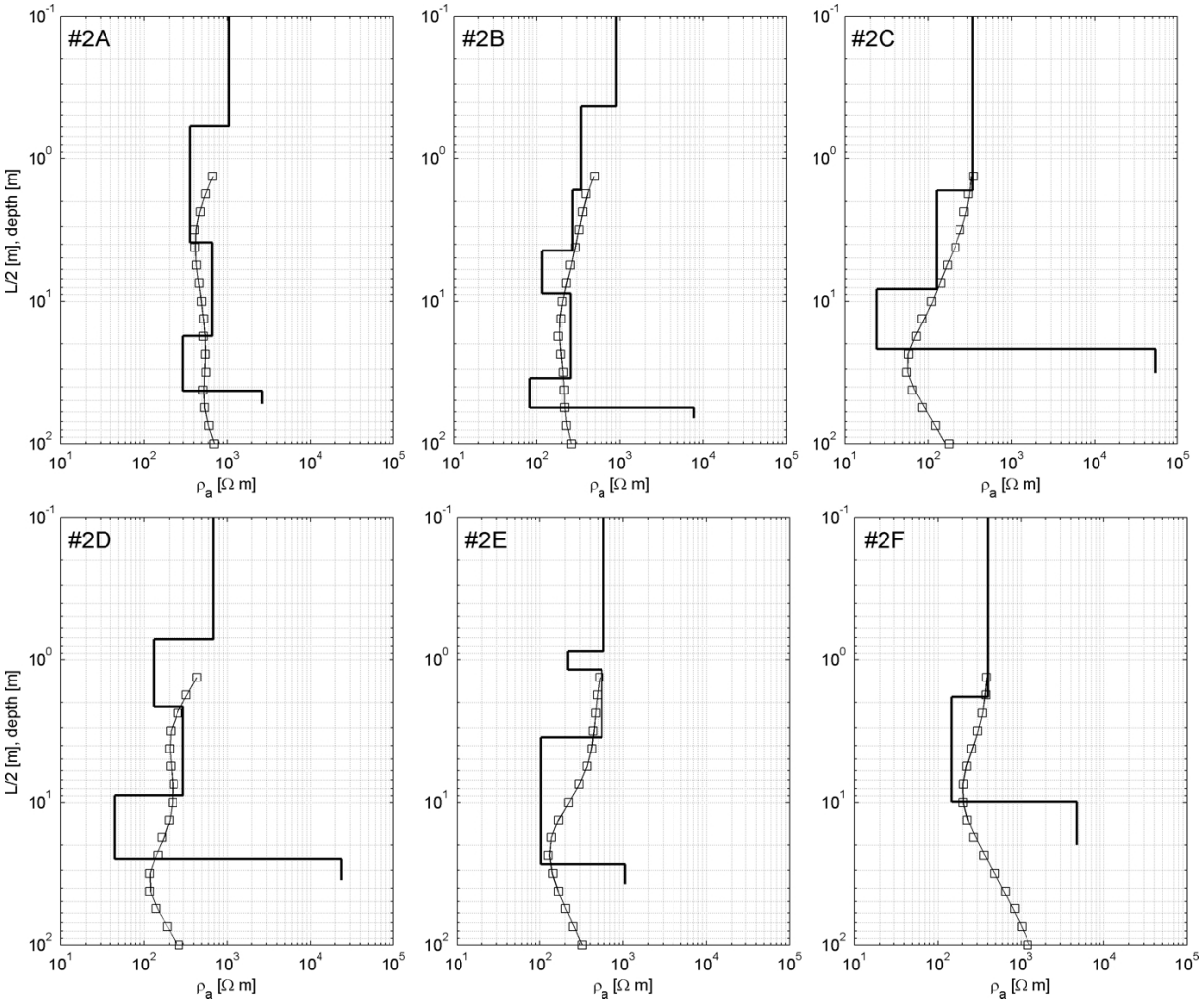

Figure 4.6: One-dimensional electrical resistivity sounding profiles in study site 2.

ted by a terrace-like flattening covered by few decimeters of debris and sand. Due to the lack of outcrops in this study site VES are the only information on the structure of the underground.

Fig. 4.7 shows the locations of VES. The electrode array of the Schlummberger configuration was expanded perpendicular to the cross valley profile to a maximum half current electrode spacing ($s/2$) of 100 m. The apparent resistivity versus electrode separation curves were modeled using three to six layer models with fitting errors ranging from 1.432 to 4.986. Insertion of multiple layers in the uppermost meter of the profile hereby yielded satisfying curve fitting in greater depths.

Relatively low variability in apparent resistivity ranging from 300 to 800 Ωm accounts

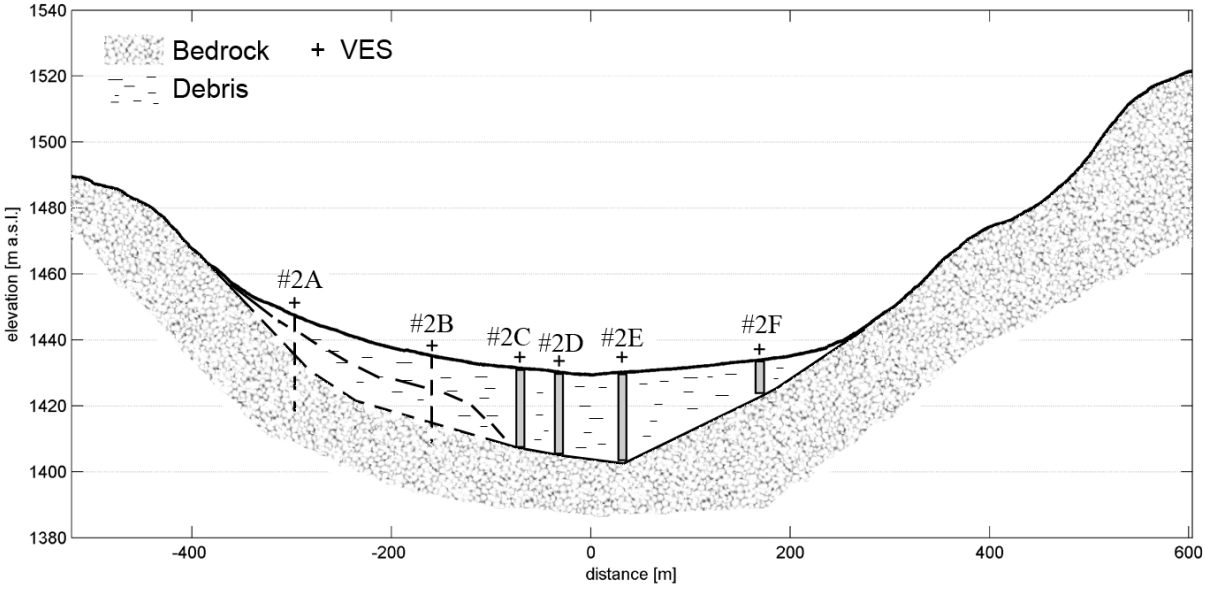

Figure 4.7: Cross valley profile, locations of one-dimensional vertical electrical soundings (VES) and interpreted subsurface relief in study site 2. Dashed lines refer to subsurface relief where VES yielded information too fuzzy to be interpreted adequate.

for VES #2A and #2B that were surveyed on the northward exposed slope (Fig. 4.6). An increase in apparent resistivity at an electrode distance of 74 m suggests a layer with decreased conductivity in 40 and 55 m depth, respectively.

VES #2C and #2D are characterized by a more variable apparent resistivity-depth relationship. A strong decrease in apparent electrical resistivity occurs in depths between 8 and 9 m below surface and suggests a layer with better electrical conductivity until a depth of about 21 to 27 m. A layer with a sharp increase in resistivity is recognized beneath. VES #2E and #2F show a less distinct highly conductive layer than VES #2C and #2E, but are also characterized by a sharp increase in resistivity in depths in 28 and 9 m below surface, respectively.

4.6 Discussion

4.6.1 Study Site 1

A timeframe of the profile in study site 1 was established by ^{14}C dates derived from humins and humic acids. The dates can be interpreted as minimum age of a deposit if (1) or-

ganic material is deposited together with inorganic material or (2) strong evidence for synsedimentary, autochthonous pedogenic origin of the material is given. Introduction and exchange of new and old carbon (biodiffusion, in situ production by roots) and the loss by microbial decomposition lead to high uncertainty in soil datings (Wang *et al.*, 1996; Madsen *et al.*, 1998; Birkeland, 1999). Yet, this problem is assumed to be less important in arid and semiarid environments (Wang *et al.*, 1996) and Pessenda *et al.* (2001) show that datings of the humin fraction compared to charcoal datings generate reliable results. Moreover, the carbonatic, cemented layer may constrict the vertical carbon exchange due to plugging (Maki *et al.*, 2007) and derogate the error of the determined ages. These arguments let us assume that the determined ages are reliable.

The prevalence of fine sand along the profile suggests the deposition of fines by aeolian processes (Pye, 1995). Relatively homogeneous beds of fines and the presence of an adjacent dune field in the vicinity of the site (Fig. 4.2) affirm this hypothesis. Moreover, the higher fraction of silt in the upper 90 cm hints at two different phases of aeolian accumulation. While the lower part reflects low distance transport by saltation and reptation and hints at the occurrence of local or regional sand sources, the upper part of the profile points at a mixture of local redeposition and mineral dust deposition. Both aeolian deposits in steppe areas have been highlighted by Grunert and Lehmkuhl (2004) and Dill *et al.* (2006).

According to the datings, the boundary between these two phases is at the Early to Mid Holocene. Dryer conditions during the Late Pleistocene to Early Holocene are found in various areas in Mongolia, but contrast findings from northern and western Mongolia (Prokopenko *et al.*, 2007; Gunin *et al.*, 1999). Such disagreements may be explained by local effects of melting water from glaciers (Walther, 1999; Walther *et al.*, 2003), but may also result from regionally varying influence of temperature on vegetation growth (Gunin *et al.*, 1999). Yet, it has been inferred from lake sediments from Ugii Nuur by Schwanghart *et al.* (2008) that there is a change towards wetter conditions in the catchment at ~ 8 ky BP and pollen analysis by Rösch *et al.* (2005) on the same core provide evidence for denser vegetation cover during this time. Hence, we suggest that the development of a denser vegetation cover during the Early to Mid Holocene both hampered sand mobilisation and favored trapping of mineral dust. The dust sources cannot be determined so far, but

ambiguous results on Mid Holocene moisture conditions in Mongolia provide evidence for a juxtaposition of adjacent regions that experience contrarian climates during this time (Gunin *et al.*, 1999; Herzschuh, 2006; Prokopenko *et al.*, 2007).

The origin of the carbonatic layer is likely connected to the aeolian accumulation of dust. Bedrock in the area is carbonate-indigent and aeolian, calcareous and Ca^{2+}-bearing deposits have been shown to play a major role in the generation of calcretes (Blümel, 1981; Besler, 1992; Birkeland, 1999). Hence, a horizontal cycle of aeolian sediment redistribution as shown by (Grunert and Lehmkuhl, 2004) for western Mongolia might also apply in the Ugii Nuur basin. After deposition, percolation and mobility in the soil profile led to the development of the carbonatic layer, that is classified as a pedogenic calcrete in the first or second state of carbonate accumulation (Wright and Tucker, 1991; Birkeland, 1999). This is supported by findings of carbonate coatings on bottom side of gravel clasts throughout the catchment and other parts of Mongolia (Klinge, 2001).

More favorable moisture conditions since Early to Mid Holocene can also be inferred from soil formation processes evidenced by the TOC and LOI profile (Fig. 4.3). While TOC contents usually tend to rapidly decrease with depth (Vallentyne, 1962; Jobbágy and Jackson, 2000; Maki *et al.*, 2007) relatively constant values are found until a depth of 1 m. This distribution partly reflects the capacity of the finer texture in the first meter to hold organic matter (Scheffer, 2002) and deep root penetration also leads to organic carbon enrichment in greater depth (Jobbágy and Jackson, 2000). Yet, high sedimentation rates caused by aeolian deposition or by soil erosion processes (Pickup and Chewings, 1988; Hill and Schütt, 2000) also lead to reduced light and oxygen availability and, thus impede microbial organic carbon decay (Lerman, 1979). Moreover, positive correlation of TOC and (heavy) metal concentrations indicates metal-organic complexes (Moore, 1973). They develop during phases of increased humidity when soil water causes locally a reducing environment and thus allows reduction, mobilisation and successive bonding in metal-organic complexes (Moore, 1973; Heikinnen, 1990). In contrast, during arid conditions prevailing oxidising conditions cause immobility of mineral iron-bondings in soils (Krauskopf, 1967; Mathess and Pekdeger, 1980). As a consequence, we interpret the vertical distribution of TOC as an indicator for soil formation in combination with high sedimentation rates of

aeolian and hillwash processes.

The findings in the sediment profile cannot be inferred from VES #1A. This is in contrast to findings of Baines *et al.* (2002) who show the applicability of electrical resistivity methods in mapping sand and gravel deposits buried by silt and clay. Obviously, the differences in electrical properties of the shallow subsurface are too ambiguous to discriminate different lithologies. Instead, lithological signals are likely to be superimposed by the higher amount of pore water that leads to a reduction of apparent resistivity in greater depths. Values around 20 to 30 Ωm indicate the presence of water with a relatively low ionic conductivity that arises from relatively low contents of dissolved salts (Mussett and Khan, 2000). An increase in apparent resistivity at 50–60 m depth can be interpreted as the boundary between the unconsolidated debris and consolidated bedrock as bedrock generally has a higher electrical resistivity than debris cover as long as the bedrock does not bare any ores (Mussett and Khan, 2000). The deepest layer, however, is only based on a few resistivity values and thus may significantly vary in depth. VES #1B exhibits higher apparent resistivities throughout the profile. Due to a lack of a directly attached borehole or profile information interpretation of VES #1B can not be validated by field evidence. However, the persistent high resistivity values in the top ten meters is interpreted as a combination of sandy to blocky debris and consolidated, but weathered bedrock which is due to its position on the slope rather dry. An increase in resistivity at 10 m depth is interpreted to be the transition to the fresh, unweathered bedrock (Dahlin, 2001).

4.6.2 Study site 2

Findings from VES surveyed at study site 2 could not be validated in the field. Here, however, especially VES #2C–F are rather distinct due to stronger contrasts in apparent resistivities. VES #2A and B show a similar behavior as VES #1B and represents the more diffuse character of slopes that might be substantially influenced by lateral variations in the underground and less distinct grain size distribution than in the valley bottoms. Interpretation of these VES in terms of layer thickness and composition are speculative and dashed lines in Fig. 4.7 account for the uncertainty in the deduction of subsurface relief. In the valley bottom strong increases in resistivity (VES #2C–F) have been recorded in 21–27

m below surface that most probably reflect the interface of debris covers and consolidated bedrock (Fig. 4.7).

4.7 Conclusions

We show that depositional environments in central Mongolia exhibit a far more complex genesis than the relatively uniform appearance of relief suggests. Since the Early to Mid Holocene input of mineral dust and fines plays a major role in the formation of the sedimentary architecture. This highlights the importance of long distance aeolian transport and probable sediment trapping by denser vegetation cover that points at wetter conditions during this time in the Ugii Nuur basin. The existence of dust sources, however, suggest dryer conditions elsewhere. This impedes the transferability of these findings on wider areas. Subjacent substrata point at the higher importance of local sand mobilization and transport that suggest higher aridity during the Late Pleistocene and Early Holocene. Furthermore, it is demonstrated that electrical resistivity tomography is applicable to quantify thicknesses of the widespread debris accumulations found. The derivation of a subsurface relief suggests that valley fillings enrobe a strong bedrock relief.

Acknowledgements

Thanks to Dr. Henry Brasse (Freie Universität Berlin) for helpful discussion and assistance by interpreting 1D electrical resistivity tomography. Thanks to Prof. Dr. Dr. hc Michael Walther (National University of Mongolia) for valuable discussions, help during field work and logistics. Thanks to Tomasz Goslar (Poznan Radiocarbon Laboratory) assisting interpretation of ^{14}C datings. Thanks to Dr. Röper for guidance and support in X-Ray diffraction analysis. Thanks to Altangerel Bat-Erdene, Judith Mahnkopf and Rikkardo Klinger and the participants of the International Field Class in 2005 and 2006 for assisting field work.